Srebric, J., Chen, Q., and Glicksman, L.R. 2000. "A coupled airflow-and-energy simulation program for indoor thermal environment studies," *ASHRAE Transactions*, 106(1), 465-476.

# A Coupled Airflow-and-Energy Simulation Program for Indoor Thermal Environment Studies (RP-927)

Jelena Srebric* ASHRAE Student Member
Qingyan Chen; Ph.D. ASHRAE Member
Leon R. Glicksman; Ph.D. ASHRAE Member

**Abstract**

Design of a thermally comfortable indoor environment requires detailed information about distribution of air velocity, air temperature, relative humidity, and mean radiant temperature and about heating/cooling load in a space. This research has developed a coupled airflow-and-energy simulation program to calculate simultaneously the distributions of indoor airflow and thermal comfort and heating/cooling load. The coupled program can take the non-uniform distributions of indoor airflow and heating/cooling load into account. The program can also provide thermal and fluid boundary conditions normally needed for room airflow calculation. This paper demonstrates the program capacity by applying the program to study the thermal environment in a house and an atrium. The coupled flow-and-energy program is recommended for the design of radiative, convective, and hybrid heating and cooling systems.

Keywords: Airflow, Air distribution, Comfort, Energy calculation, Modeling, Space environment

## Introduction

Air temperature, relative humidity, air velocity, and environmental radiant temperature are the four most important parameters for thermal comfort (ASHRAE 1992). In an indoor space with radiative, convective, and hybrid heating and cooling systems, the distribution of these parameters is non-uniform and the thermal comfort level varies with location. Many current comfort designs use a single value of air temperature and velocity to represent thermal comfort in a room. A single value is not sufficient because the distributions of air temperature and velocity may not be uniform. To design an acceptable indoor thermal environment, designers need a tool that can predict the distributions of thermal comfort parameters, such as air velocity and temperature.

The assumption of a uniform distribution of room air temperature could also lead to an error in estimating heating/cooling load in a building (Chen and Kooi 1988). This is especially evident in large spaces with convective, radiative, and hybrid heating and cooling systems. In the past few years, many investigations have studied the interconnections between indoor airflow computation and building energy analysis. For example, Nielsen and Tryggvason (1998) used a computational-fluid-dynamics (CFD) program and an energy analysis program to improve the computational accuracy of the airflow, air quality, and energy flow in a building. Onishi et al. (1988) discussed their effort to reduce computing time when a CFD program is used to calculate unsteady room airflow and thermal environment.

Our study has developed a coupled airflow-and-energy program to predict thermal comfort and heating/cooling load in a space with a non-uniform indoor thermal environment.

* Jelena Srebric is a Ph.D. Candidate, Qingyan (Yan) Chen is an Associate Professor, and Leon R. Glicksman is a Professor at the Building Technology Program, Department of Architecture, Massachusetts Institute of Technology, MA.

The following section presents the fundamentals of the coupled program. Later sections discuss the program capacity by applying it to study indoor thermal environment in a house and an atrium.

**The Program Fundamentals**

To predict the indoor thermal environment, one needs to determine air velocity, temperature and relative humidity in a room. The prediction is done in the coupled airflow-and-energy program by using the CFD technique that solves the following time-averaged Navier-Stokes equations for the conservation of mass, momentum, and energy:

Mass continuity:

$$\frac{\partial V_i}{\partial x_i} = 0 , \tag{1}$$

where $V_i$ = the mean velocity component in $x_i$-direction and

$x_i$ = the coordinate (for i=1, 2, 3, $x_i$ corresponds to three perpendicular axes).

Momentum conservation:

$$\frac{\partial \rho V_i}{\partial t} + \frac{\partial \rho V_i V_j}{\partial x_j} = -\frac{\partial p}{\partial x_i} + \frac{\partial}{\partial x_j}\left[\mu_{eff}\left(\frac{\partial V_i}{\partial x_j} + \frac{\partial V_j}{\partial x_i}\right)\right] + \rho\beta(T_o - T)g_i , \tag{2}$$

where $\rho$ = air density

$V_j$ = velocity component in $x_j$-direction

t = time

p = pressure

$\mu_{eff}$ = effective viscosity

$\beta$ = thermal expansion coefficient of air

$T_o$ = temperature at a reference point

T = temperature and

$g_i$ = gravity acceleration in i-direction.

The last term on the right side of the equation is the buoyancy term.

The turbulent influences on the flow are lumped into the effective viscosity as the sum of the turbulent viscosity, $\mu_t$, and laminar viscosity, $\mu$:

$$\mu_{eff} = \mu_t + \mu . \tag{3}$$

The coupled program has used a single algebraic function (a zero-equation model) to express the turbulent viscosity as a function of local mean velocity, V, and a length scale, l (Chen and Xu 1998):

$$\mu_t = 0.03874\ \rho\ V\ l , \tag{4}$$

where l = length scale, the distance to the closest surface of the enclosure (Chen and Xu 1998).

Energy balance:

$$\frac{\partial \rho T}{\partial t} + \frac{\partial \rho V_j T}{\partial x_j} = \frac{\partial}{\partial x_j}\left(\Gamma_{T,eff}\frac{\partial T}{\partial x_j}\right) + \frac{q}{c_p} , \tag{5}$$

where $\Gamma_{T,eff}$ = effective turbulent diffusion coefficient for T

q = heat source and

$c_p$ = specific heat.

Further,

$$\Gamma_{T,eff} = \frac{\mu_{eff}}{Pr_{eff}} , \qquad (6)$$

where $Pr_{eff} = 0.9$, the effective Prandtl number.

By solving Equations (1) to (6), one could obtain flow information. However, boundary conditions are necessary for the mathematical solution of the conservation equations. Typical boundary conditions in a room are wall surface temperature, air supply velocity and temperature from a diffuser, etc. These boundary conditions can be obtained from an energy analysis program. In this study, the energy analysis program, ACCURACY (Chen and Kooi 1988), was used. The energy simulation program calculates hourly heating/cooling load based on the room energy balance method:

$$\sum_{i=1}^{N} q_{i,c} A_i + Q_{lights} + Q_{people} + Q_{appliances} + Q_{inf\,iltration} - Q_{heat\_extraction} = \frac{\rho V_{room} C_p \Delta T}{\Delta t} , \qquad (7)$$

where $\sum_{i=1}^{N} q_{i,c} A_i$ = convective heat transfer from enclosure surfaces to room air

$q_{i,c}$ = convective heat flux from the enclosure surface i

N = number of enclosure surfaces

$A_i$ = area of surface i

$Q_{lights}$, $Q_{people}$, $Q_{appliances}$, and $Q_{infiltration}$ = cooling loads from lights, people, appliances and infiltration, respectively, determined by ASHRAE methods (ASHRAE 1997)

$Q_{heat\_extraction}$ = heat extraction rate by HVAC device

$\frac{\rho V_{room} C_p \Delta T}{\Delta t}$ = room air energy change

$\rho$ = air density

$V_{room}$ = room volume

$C_p$ = specific heat

$\Delta T$ = temperature change of room air and

$\Delta t$ = sampling time interval.

The convective heat flux from surface i, $q_{i,c}$, as shown in Figure 1(a) is calculated through the following energy balance equations for a wall, ceiling, floor, roof, or slab:

$$q_i + q_{i,t} = \sum_{k=1}^{N} q_{ik} + q_{i,c} , \qquad (8)$$

where $q_i$ = conductive heat flux on surface i

$q_{i,t}$ = transmitted solar heat flux re-absorbed by surface i and

$q_{ik}$ = emitted radiative heat flux from surface i to surface k.

The program determines $q_i$ by Z-transfer functions. The radiative heat flux is

$$q_{ik} = h_{ik,r} (T_i - T_k) , \qquad (9)$$

where $h_{ik,r}$ = radiative heat transfer coefficient between surfaces i and k

$T_i$ = temperature of interior surface i and

$T_k$ = temperature of interior surface k.

The convective heat flux is

$$q_{i,c} = h_c (T_i - T_{air}) , \qquad (10)$$

where $h_c$ = convective heat transfer coefficient and

$T_{air}$ = room air temperature.

The convective heat transfer coefficient is determined from the following equation in the room

airflow computation, which is similar to the Reynolds analogy:

$$h_c = \frac{\mu_{eff}}{Pr_{eff}} \frac{C_p}{\Delta x_j} \ , \tag{11}$$

where $\Delta x_j$ is the distance between the surface and the location where $T_{air}$ is taken.

Many existing energy simulation programs assume $T_{air}$ to be uniform in the entire indoor space. This assumption is appropriate for a room with a perfect mixing ventilation system where the room air temperature is relatively uniform. However, a single temperature is not good for rooms with convective, radiative, and hybrid heating/cooling systems. This is because the non-uniform temperature distribution in the rooms can have a major impact on the heating/cooling load as determined by Equation (10). The air temperature at the boundary layer of a wall is an important factor for the heat transfer through convection in the air-wall interface. This study uses the air temperature at the first flow grid from a wall surface ($T_{i,air}$ in Figure 2(b)) as the $T_{air}$. If the air temperature in the center of the occupied zone is controlled to be $T_{room}$, Equation (10) becomes:

$$\begin{aligned} q_{i,c} &= h_{i,c} (T_i - T_{i,air}) \\ &= h_{i,c}(T_i - T_{room}) - h_{i,c} \Delta T_{i,air} \ , \end{aligned} \tag{12}$$

where $\Delta T_{i,air} = T_{i,air} - T_{room.}$

The $T_{i,air}$ is obtained from the CFD simulation as shown in Figure 2(a).

For a window shown in Figure 1(b), the following energy balance equation is used:

$$q_i + q_{i,s} + q_{i,t} = \sum_{k=1}^{N} q_{ik} + q_{i,c} \ , \tag{13}$$

where $q_i$ = conductive heat flux on window i

$q_{i,s}$ = inward heat flux of the absorbed solar radiation by window i

$q_{i,t}$ = transmitted solar heat flux re-absorbed by window i and

$q_{ik}$ = emitted radiative heat flux from window i to room surface k.

The coupled program calculates $q_i$, $q_{i,s}$, and $q_{i,t}$ according to solar position and window material properties. The $q_{ik}$ and $q_{i,c}$ are determined in the same way as those for walls.

Let

$q_{i,in} = q_i + q_{i,t}$ for walls, ceilings, floors, slabs, etc. and

$q_{i,in} = q_i + q_{i,s} + q_{i,t}$ for windows.

Then the room energy balance equations can be established:

$$[\mathbf{H}]\,[\mathbf{T}] = [\mathbf{q}] + [\mathbf{h}\,\Delta\mathbf{T}] \ , \tag{14}$$

where

$$[\mathbf{H}] = \begin{bmatrix} h_{1,c} + \sum_{k=1}^{N} h_{1k,r} & -h_{12,r} & \cdots & -h_{1N,r} \\ -h_{21,r} & h_{2,c} + \sum_{k=1}^{N} h_{2k,r} & \cdots & -h_{2N,r} \\ \cdots & \cdots & \cdots & \cdots \\ -h_{N1,r} & \cdots & -h_{NN-1,r} & h_{N,c} + \sum_{k=1}^{N} h_{Nk,r} \end{bmatrix} \tag{15}$$

$$[\mathbf{T}] = \begin{bmatrix} T_1 \\ T_2 \\ \cdots \\ T_N \end{bmatrix} \tag{16}$$

$$[\mathbf{q}] = \begin{bmatrix} q_{1,in} + h_{1,c} T_{room} \\ q_{2,in} + h_{2,c} T_{room} \\ \cdots \\ q_{N,in} + h_{N,c} T_{room} \end{bmatrix} \quad (17)$$

$$[\mathbf{h}\ \Delta\mathbf{T}] = \begin{bmatrix} h_{1,c} \Delta T_{1,air} \\ h_{2,c} \Delta T_{2,air} \\ \cdots \\ h_{N,c} \Delta T_{N,air} \end{bmatrix} . \quad (18)$$

By solving Equations (7) to (18) together, the surface temperatures of room enclosure, $T_i$, and heat extraction rate (heating/cooling load) can be obtained. The $T_i$ and heat extraction rate are the boundary conditions for Equations (1) to (6).

The coupled program uses the outputs from the coupled airflow-and-energy simulations to determine the distribution of thermal comfort with the ASHRAE comfort model (ASHRAE 1997):

$$PPD = 100 - 95\exp(-0.03353PMV^4 - 0.2179PMV^2) \ [\%] \ , \quad (19)$$

where PPD = Predicted percentage dissatisfied and

PMV = Predicted mean vote.

The predicted mean vote, PMV, in the equation is determined by:

$$PMV = 3.155\ [0.303\ \exp(-0.114\ M) + 0.028]\ L \quad \text{(I-P)} \quad (20a)$$

$$PMV = [0.303\exp(-0.036M) + 0.028]\ L \quad \text{(SI)} \quad (20b)$$

where M = Metabolism and

L = Load.

The M and L are the functions of air temperature, air velocity, and environmental temperature. The distributions of air temperature and velocity are determined by Equations (2) and (5), and the environmental temperature distribution by Equation (14). Then the coupled program calculates the distribution of PPD in a space.

Equations (1) to (20) form the fundamentals of the coupled airflow-and-energy program. Figure 3 illustrates the program structure. The numeric scheme used is quasi-steady to save computing time. The surface temperature and heat extraction rates in the current hour are used to calculate the air velocity, air temperature and heat transfer coefficients in the current hour. The air temperature and heat transfer coefficients in the current hour are used to determine the surface temperature and heat extraction in the next hour.

**Simulation Results**

The coupled program has been validated by the experimental data obtained from an environmental chamber and from the literature. The validation results appear in the references (Srebric et al. 1999, Chen et al. 1999, Chen and Kooi 1988). The coupled program has been used to simulate indoor thermal environment in a house (Hanibuchi and Hokoi 1996), an atrium (Hiramatsu et al. 1996), an aircraft hanger (Notarianni and Davis 1993), a large office with partition walls (Yuan et al. 1999), and a factory with individual workstations (Yuan et al. 1999). A more completed report is now available (Chen et al. 1999). The remaining sections of the paper show some of the results for the house and atrium to demonstrate the capacity of the coupled program.

For the analysis of the dynamic performance of the coupled airflow-and-energy program,

the study used typical meteorological year (TMY) data sets derived from the 1961 - 1990 national solar radiation database. Since the purpose of the study is to demonstrate the capacity of the coupled program, the investigation used Boston weather data and focused on only two typical days in a year: January 7 in the winter and July 8 in the summer.

**Simulation of indoor thermal environment in a house**

The house used in the simulation exercise, shown in Figure 4, is 6.0 m (20 ft) long, 4.0 m (13 ft) wide, and 2.5 m (8 ft) high. For simplicity, the house was assumed to be empty and had no partitions. The house was selected because Hanibuchi and Hokoi (1996) measured air velocity and temperature distribution in the house under a steady state condition. The data was used to validate the coupled program (Chen et al. 1999). For the demonstration purpose, the materials used for the ceiling, floor, walls were changed from those used in the experimental rig to be more appropriate as shown in Table 1. An air-conditioner was used to heat the house. The air-conditioner was installed above the window on Wall-3.

The calculation assumed that the house was conditioned 24 hours per day and the indoor air temperature was set at 25$^{o}$C (77$^{o}$F). Since an air-conditioner was used, the airflow rate from the air conditioner was constant (420 m$^{3}$/h, 250 cfm), which corresponds to an air change rate of 7 ach. Then the air supply temperature at each hour was determined from the heat extraction rate and the airflow rate.

The windows had no shading device. The house had no internal heat gain/loss. The filtration was assumed to be zero and the air temperature in the basement to be 20$^{o}$C (68$^{o}$F) all year around.

Figure 5(a) shows total amount of direct and diffuse solar radiation received on a horizontal surface. The outdoor air temperatures in the winter and summer days are illustrated in Figure 5(b). Figure 5(c) shows the heat extraction rate (positive means cooling and negative implies heating) computed by the coupled program for the house. During the winter day, the house needs heating all the time, because of the low outside air temperature and small solar radiation. In the very early morning hours, the house needs heating in the summer. This is due to no internal heat gains in the house and relatively low outdoor air temperature. The solar radiation in the daytime reduces the heating load on the winter day, but it increases the cooling load on the summer day. During the summer afternoon, the cooling load increases significantly due to the solar radiation from the west window.

Although the computations of the indoor thermal environment in the house have been carried out hour by hour for the winter and summer days, the results are presented here only for 4 am, 8 am and 12 noon in the winter day. Figures 6 to 8 show the air velocity, temperature, and PPD distributions in two sections in the house, respectively. The air was supplied at angle of 40$^{o}$ downward from the air conditioner in order to achieve better mixing, because of the strong buoyant effect from the air conditioner. Figure 6 illustrates a counter-clockwise air circulation in the house created by the jet flow from the air-conditioner. The air velocity near the diffuser was significantly higher than that in the other part of the house. Although the outdoor air temperature and solar radiation varied during the day, the indoor airflow patterns looked similar.

However, the difference in the temperature distributions is more evident. At 4 am, the outdoor air temperature was low and the solar radiation is zero, the supply air temperature was the highest in order to heat the house to the set point temperature. The supply air temperature decreased when the outdoor air temperature increased and the solar radiation entered the windows. Even with the mixing ventilation and downward supply, the air temperature in the

house was not uniform. If the house were heated by a convector, a baseboard heater, or other convective, radiative, and hybrid heating systems, there would be a large air temperature stratification in the house.

As shown in Figure 8, the comfort level in the house was generally good. Except in the area near the air conditioner, the PPD is less than 10% in most parts of the house. In practice, a house may not be empty and may have different heat sources/sinks, so the PPD distribution would not be as uniform as the house studied.

**Simulation of indoor thermal environment in an atrium**

The atrium used here is a full-scale test facility in Japan (Hiramatsu et al. 1996). The experimental data have been used to validate the coupled flow-and-energy program (Chen at al. 1999). Many researchers have used this atrium as a reference case. Figure 9 illustrates the appearance and size of the atrium. The ceiling and the south, west and east walls of the atrium are glazed. The floor and the north wall are insulated. The atrium is empty and had no partitions. In addition, the atrium is assumed to have no internal heat gain/loss and filtration in the simulation. The building materials used for the present study, as Table 2 shows, could be different from the original design. Since this case is used to demonstrate the coupled program capacity, the difference should not be a concern. Similar to the previous case, our study has used the TMY weather data for Boston.

The present investigation assumes that the atrium is only conditioned between 8 am and 6 pm. The air temperature is controlled at 23$^{o}$C (73.4$^{o}$F) in the winter day and 25$^{o}$C (77$^{o}$F) in the summer day, as Figure 10(a) illustrates. The ventilation system used for air-conditioning is a constant air volume system. The air change rate is fixed at 15 ach. The ventilation rate is very large because of the large heat extraction rates in the atrium. The inlet air temperature varies with time and is determined by the corresponding heat extraction rate and ventilation rate.

In the winter day, the atrium air temperature in the early morning hours was close to the outdoor air temperature. In the evening, the atrium air temperature decreased but was still higher than the outdoor air temperature, due to the thermal capacity of the north wall and the floor. The atrium air temperature during the non-conditioned hours in the summer day was very close to that during the conditioned period. This is because the outdoor air temperature during the non-conditioned period was close to the setting point. The large cooling load due to solar radiation during the daytime was immediately removed by the air conditioning system.

Figure 10(b) shows the heat extraction rate (positive means cooling and negative implies heating) in the atrium. Since the atrium was conditioned from 8 am to 6 pm, the heat extraction rate was zero before 8 am and after 6 pm. Obviously, because of the large glazed area, the heat extraction rate is very sensitive to the solar radiation and outdoor air temperature.

Figures 11 to 13 show the air velocity, temperature, and PPD distributions at 4 am, 8 am, and 12 noon in the atrium during the summer day, respectively. At 4 am, the atrium was not conditioned. Figure 11 shows that the air movement due to natural convection was very weak, because the air temperature difference between indoors and outdoors was small. The air temperature was 22.8$^{o}$C (73$^{o}$F). The air temperature distribution was rather uniform as shown in Figure 12. As a result, Figure 13 shows that the corresponding PPD distribution at 4 am was uniform.

At 8 am, the air-conditioning systems started to work, but the heat extraction was not very high (1090 W, 3719 Btu/h). The supply air temperature was 23.4$^{o}$C (74$^{o}$F). Since the airflow rate is rather high, the jet could reach to the opposite wall as illustrated in Figure 11. Due

to the mechanical ventilation, the air velocity in the atrium at 8 am was higher than that at 4 am. Figure 12 shows that the temperature distribution in the atrium was still uniform because of the small temperature difference between the atrium air and the supply air. However, the PPD distribution was not uniform in the jet area as can be seen from Figure 13. Nevertheless, the PPD distribution in the occupied zone is still uniform.

At the noon, the heat extraction rate was 14,412 W (49,171 Btu/h). The corresponding air supply temperature was 4$^{o}$C (39$^{o}$F). Although the buoyancy effect became very strong, the inertial momentum force was much stronger. Hence, the jet can still reach the south glass (Figure 11). Figure 12 indicates the temperature distribution in the atrium is not very uniform, although the system is still regarded as mixing. The non-uniform mixing of air velocity and temperature led to a non-uniform PPD distribution even in the occupied zone, as shown in Figure 13.

**Discussion**

The non-uniform air velocity and temperature distributions have a significant impact on the calculation of the heat extraction rate. With a single temperature and convective heat transfer coefficient, the error can be as high as 30%, when Chen and Kooi (1988) compared their calculated cooling load with the experimental data. Good agreement was achieved, when the non-uniform air temperature distribution and correct heat transfer coefficient were used in the cooling load calculation. This can be easily seen from Equation (14), which indicates that both the temperature distribution and convective heat transfer coefficients play important roles in the calculation of the heat extraction rate. It is therefore very important to couple an airflow program with an energy analysis program to obtain more accurate results. Nielsen and Tryggvason (1998) confirmed that an interconnection between a CFD program and a building energy performance simulation program would improve both the energy consumption data and the prediction of thermal comfort and air quality in a selected area of a building.

Chen et al. (1995) used a conjugate heat transfer model to calculate the dynamic performance of the building system and indoor thermal environment. The model solves the energy equation in the CFD model for the heat conduction in a wall. The conjugate heat transfer model is accurate, but the computing time is very high due to the discontinuity of the density at the solid-air interface. The current method is much faster, since it calculates room airflow and heat conduction in the building enclosure separately. It takes about three hours in a Pentium II PC to calculate hour by hour the airflow and heat extraction rate in the house and atrium for the winter or summer day. It would still take too much computing time if the hour-by-hour simulation were required for a whole year. However, in design practice, it may not be necessary to conduct hour by hour simulation of the indoor airflow for a whole year. A typical day in a season would provide a designer sufficient information. Therefore, the tool developed in the research project is very useful.

**Conclusions**

The aim of the research was to couple airflow simulation with energy analysis in a building. A coupled airflow-and-energy program has been developed to calculate the hour-by-hour distributions of airflow, heating/cooling load, and thermal comfort in a space. This paper demonstrates the program's capacity by applying the program to a house and an atrium. The results show that the coupled program is capable of studying the dynamic airflow, heating/cooling load, and thermal comfort simultaneously in a space on a personal computer.

The results show that indoor air distribution in mixing ventilation may not be uniform.

The impact of the non-uniform distribution of indoor air can be considered in the calculation of heating/cooling load by the coupled program. Since radiative, convective, and hybrid heating and cooling systems for a building may create a non-uniform distribution of indoor air, the coupled program is useful to help a designer to design an acceptable indoor thermal environment and to size suitable HVAC equipment.

**Acknowledgement**

The study was supported by ASHRAE RP-927 and National Science Foundation grant CMS-9623864.

**References**

ASHRAE. 1992. *ASHRAE Standard 55-1992: Thermal Environmental Conditions on Human Occupancy*, ASHRAE, Atlanta.

ASHRAE. 1997. *ASHRAE Handbook - Fundamentals*. ASHRAE, Atlanta.

Chen, Q. and Kooi, J. v. d. 1988. "ACCURACY - a computer program for combined problems of energy analysis, indoor airflow and air quality," *ASHRAE Trans*. 94(2): 196-214.

Chen, Q., and Xu, W. 1998. "A zero-equation turbulence model for indoor airflow simulation," *Energy and Buildings*, 28(2): 137-144.

Chen, Q., Peng, X. and Paassen, A.H.C. van, 1995. "Prediction of room thermal response by CFD technique with conjugate heat transfer and radiation models," *ASHRAE Trans.*, 101(2): 50-60.

Chen, Q., Glicksman, L.R. and Srebric, J. 1999. "Simplified methodology to factor room air movement and the impact on thermal comfort into design of radiative, convective and hybrid heating and cooling systems," Final Report for ASHRAE RP-927, Department of Architecture, Massachusetts Institute of Technology, Cambridge, MA, USA.

Hanibuchi, H. and Hokoi, S. 1996. "An analysis of velocity and temperature fields in a room heated by a room air-conditioner," *Proc. of ROOMVENT '96*, Vol. 1, pp. 445-452.

Hiramatsu, T., Harada, T., Kato, S., Murakami, S., and Yoshino, H. 1996. "Study of thermal environment in experimental real-scale atrium," *Proc. of ROOMVENT '96,* Vol. 1, pp. 523-529.

Nielsen, P.V. and Tryggvason, T. 1998. "Computational fluid dynamics and building energy performance simulation," *Proc. of ROOMVENT '98*, Vol. 1, Stockholm.

Notarianni, K.A. and Davis, W.D., 1993. "The use of computer models to predict temperature and smoke movement in high bay spaces," National Institute of Standards and Technology, Report Number: NISTIR 5304.

Onishi, J., Kogal, S., Mizuno, M., Takeya, N. Kitagawa, K. 1998. "Computer effort saving methods in unsteady calculations of room airflows, and thermal environments," *Proc. of ROOMVENT '98*, Vol. 1, Stockholm.

Srebric, J., Chen, Q., and Glicksman, L.R. "Validation of a zero-equation turbulence model for complex indoor airflows," *ASHRAE Transactions*, 105(2).

Yuan, X., Chen, Q., and Glicksman, L.R. 1999. "Performance evaluation and design guidelines for displacement ventilation," *ASHRAE Transactions*, 105(1).

Table 1. The materials used for the house.

| Enclosure | Layer | Thickness (m) | Specific heat (J/kg K) | Density ($kg/m^3$) | Conductivity (W/m K) |
|---|---|---|---|---|---|
| Floor | 1 | 0.10 | 840 | 2243 | 1.731 |
| Ceiling | 3 | 0.10<br>0.10<br>0.01 | 840<br>500<br>1215 | 1600<br>190<br>545 | 0.52<br>0.046<br>0.12 |
| Walls | 3 | 0.10<br>0.10<br>0.01 | 840<br>1210<br>840 | 2082<br>55<br>721 | 1.3<br>0.027<br>0.72 |
| Windows | 2 (double-glazing) | The reflection index of the glass is 1.52, the thickness of the glass is 6 mm, and the absorptivity of the glass is 0.018. | | | |

Table 2. The materials used for the atrium.

| Enclosure | Layer | Thickness (m) | Specific heat (J/kg K) | Density ($kg/m^3$) | Conductivity (W/m K) |
|---|---|---|---|---|---|
| Floor | 1 | 0.10 | 840 | 2243 | 1.731 |
| North wall | 3 | 0.10<br>0.10<br>0.01 | 840<br>1210<br>840 | 2082<br>55<br>721 | 1.3<br>0.027<br>0.72 |
| Ceiling glazing | 1 | The reflection index of the glass is 1.52, the thickness of the glass is 6 mm, and the absorptivity of the glass is 0.018. | | | |
| South, east, and west glazing | 1 | The same as the ceiling. | | | |

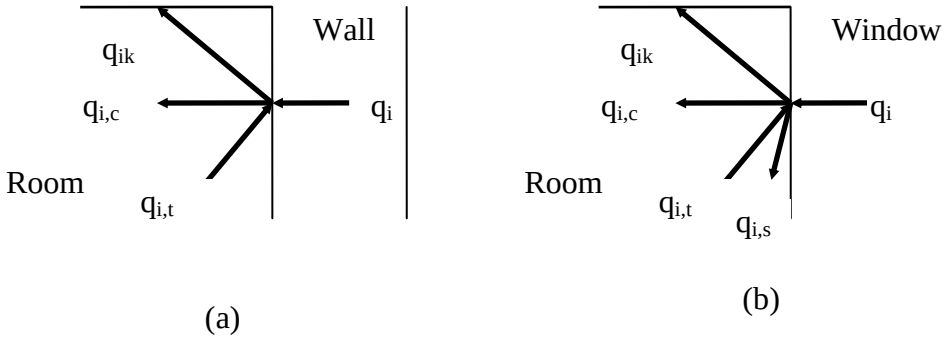


Figure 1. Energy balance on the interior surface of building enclosure. (a) for a wall, ceiling, floor, roof, or slab, (b) for a window.

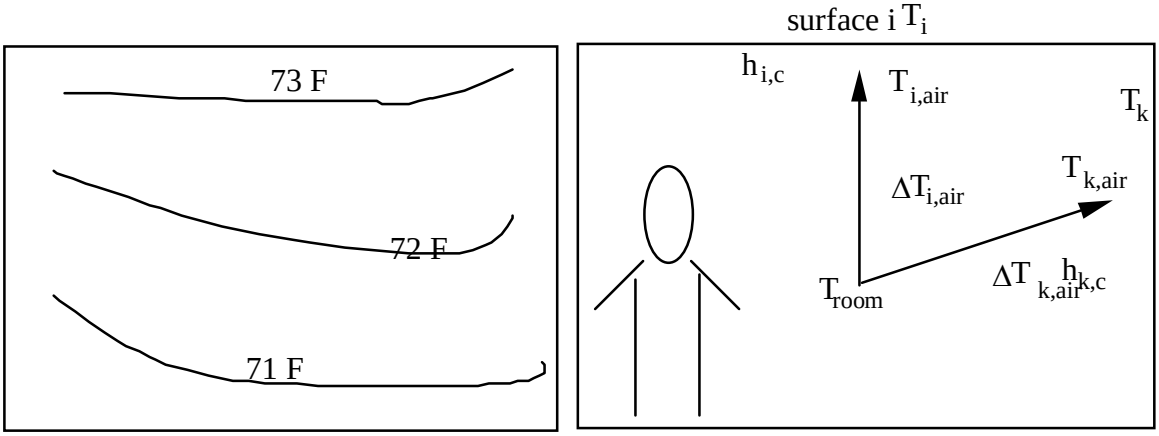


(a) Temperature computed by the flow program (b) Temperature used in the energy program

Figure 2. Schematic presentation of the coupling between airflow-and-energy calculations.

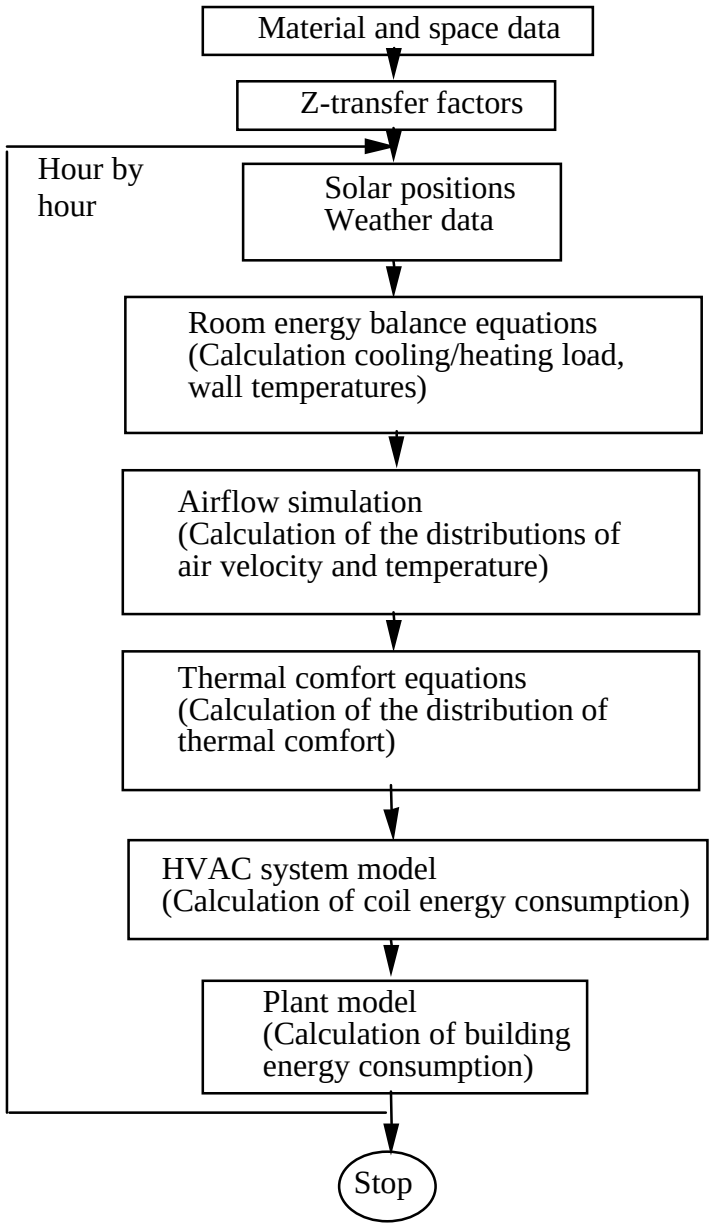


Figure 3. The structure of the coupled airflow-and-energy program.

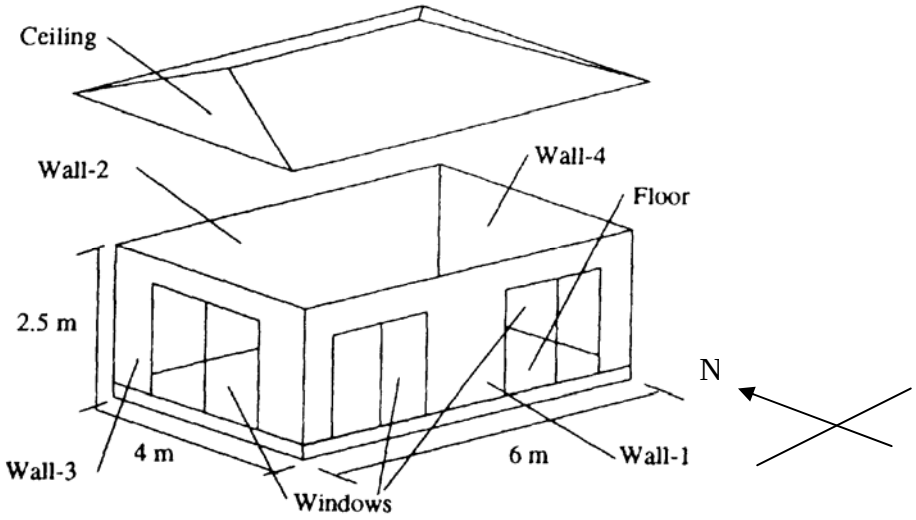


Figure 4. The sketch of the house.

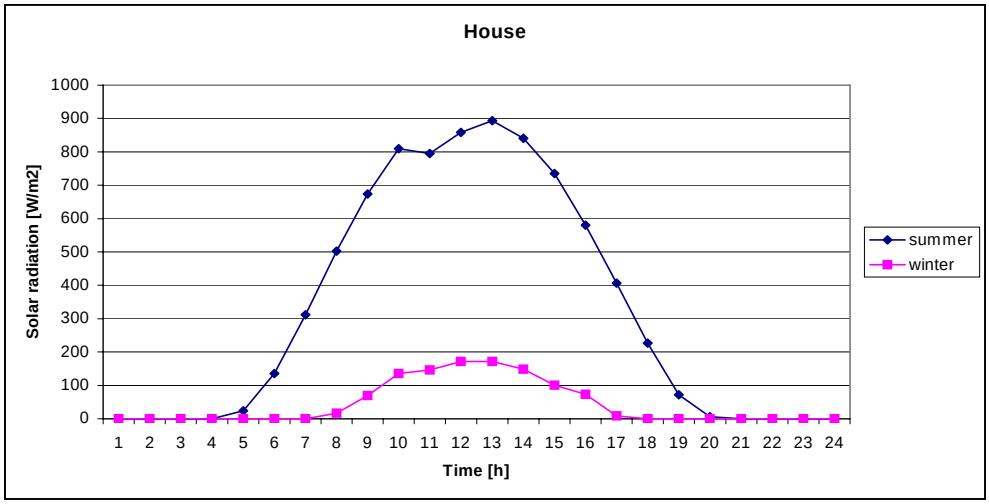


(a)

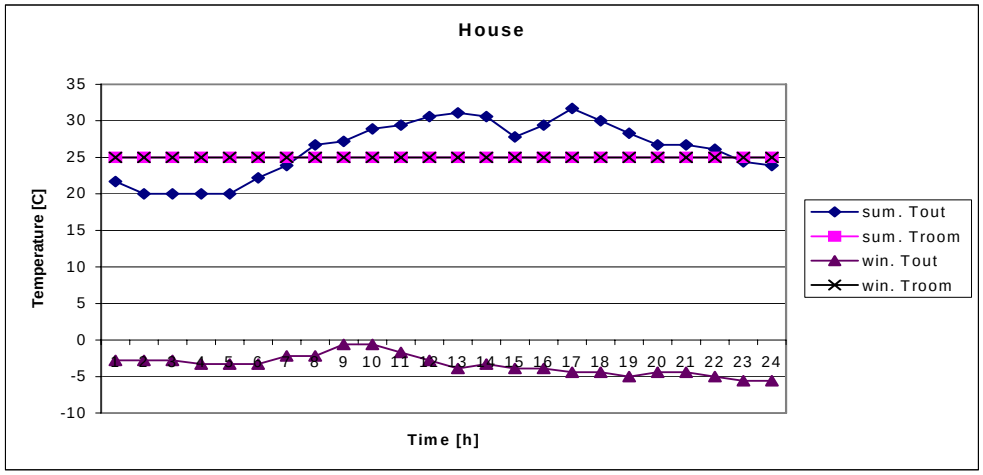


(b)

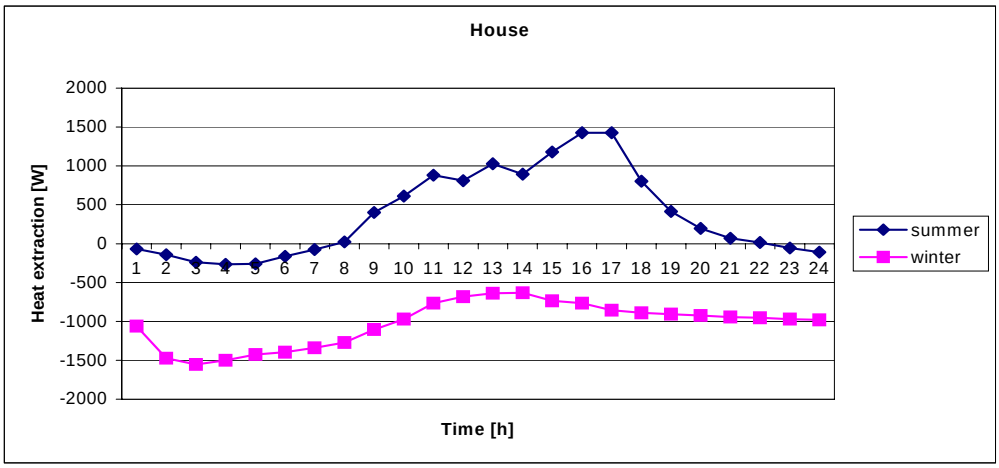


(c)

Figure 5. The climate data and results calculated by the coupled program for the house for the winter and summer days. (a) Outdoor solar radiation, (b) indoor and outdoor air temperature, (c) heat extraction rate.

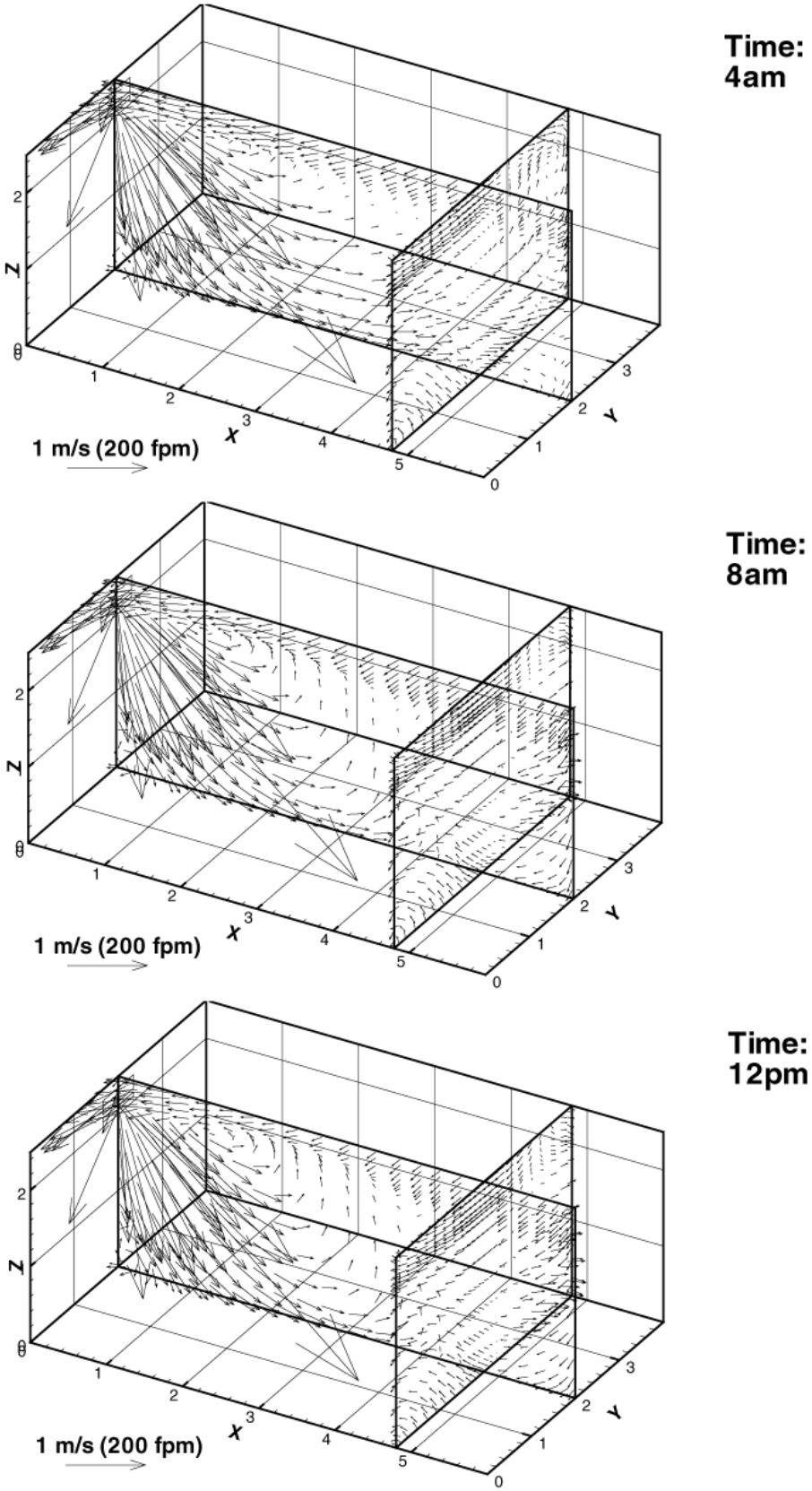


Figure 6. The computed air velocity distributions for the house during the winter day.

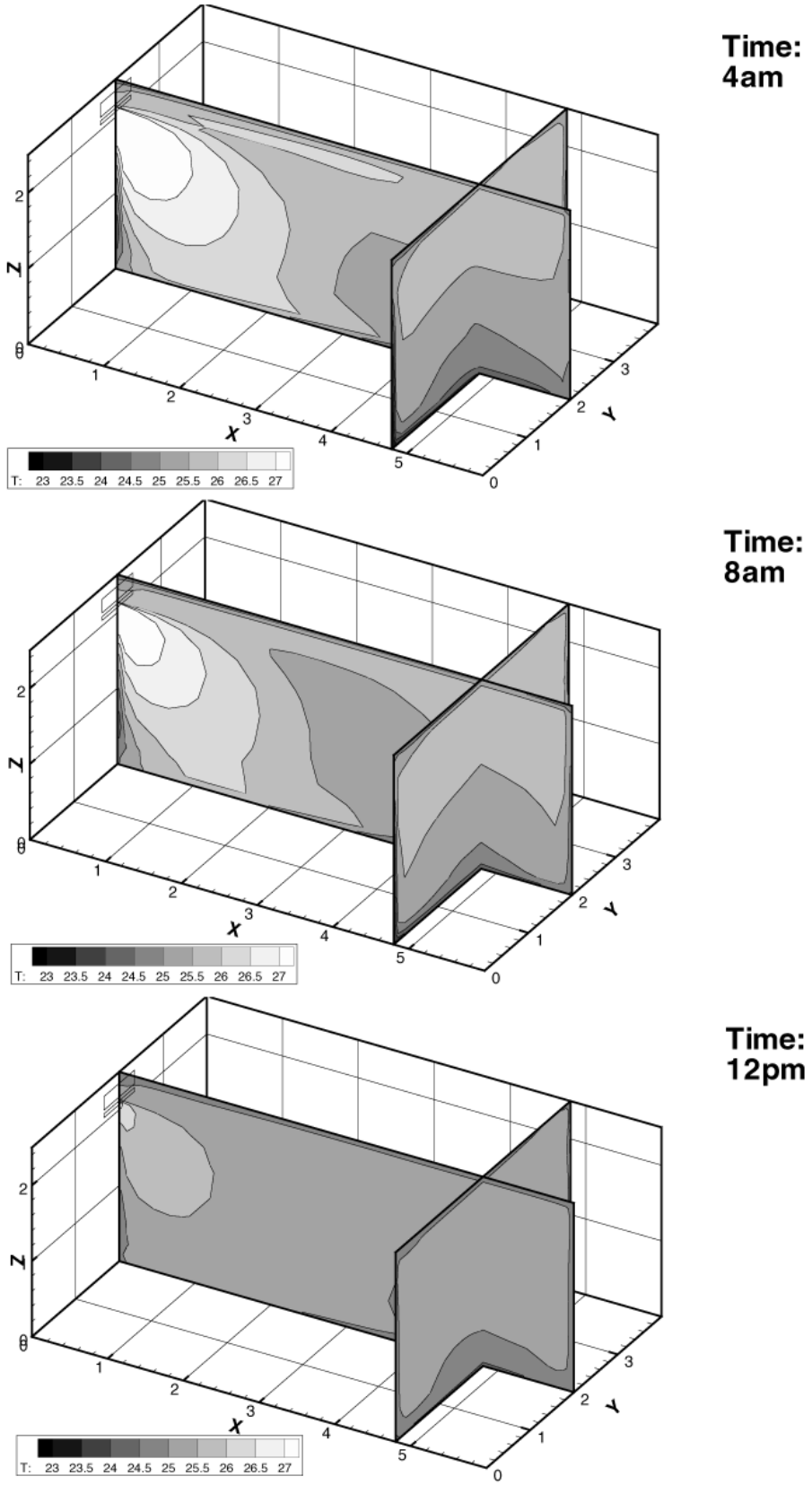


Figure 7. The computed air temperature distributions for the house during the winter day.

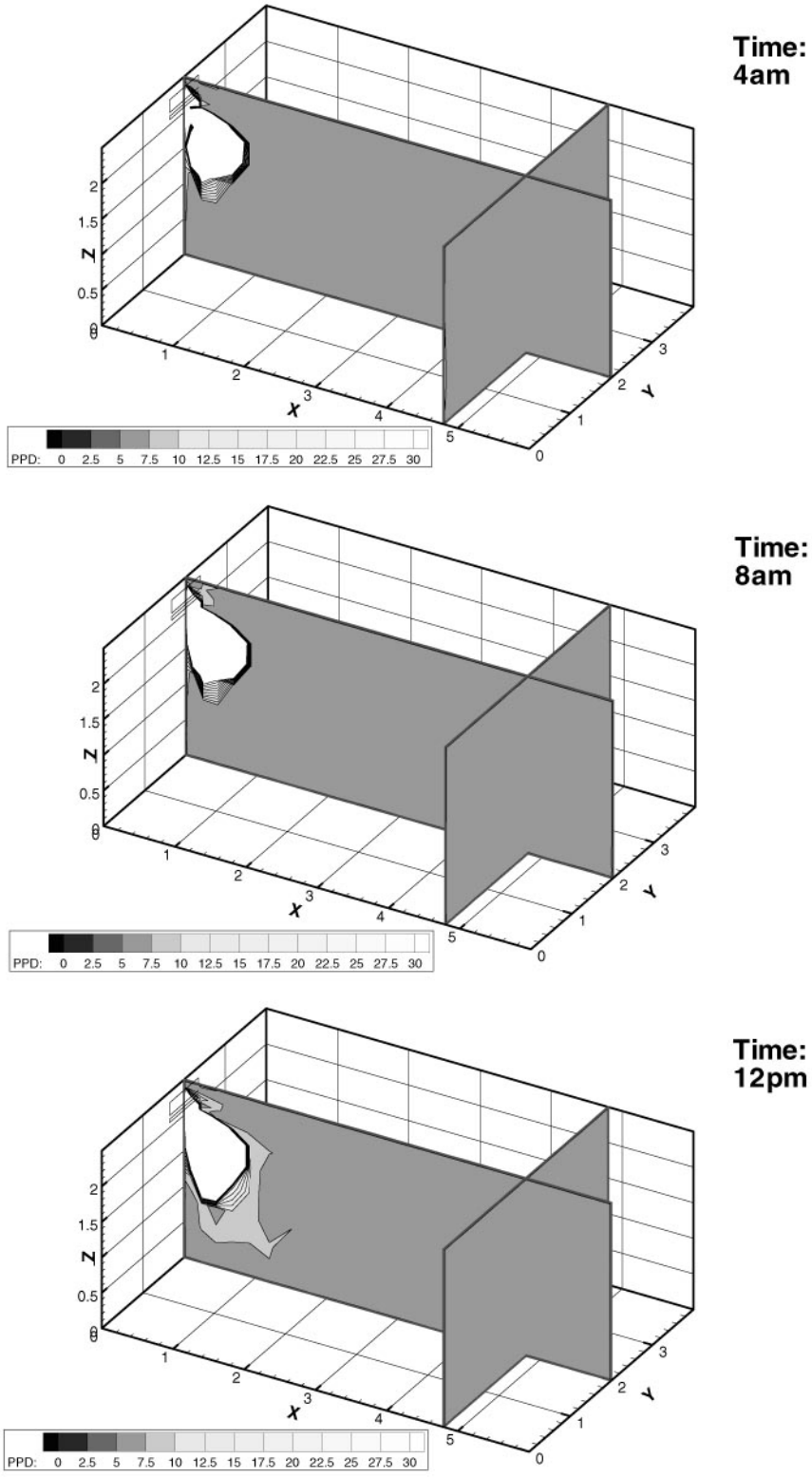


Figure 8. The predicted percentage dissatisfied distributions in the house during the winter day.

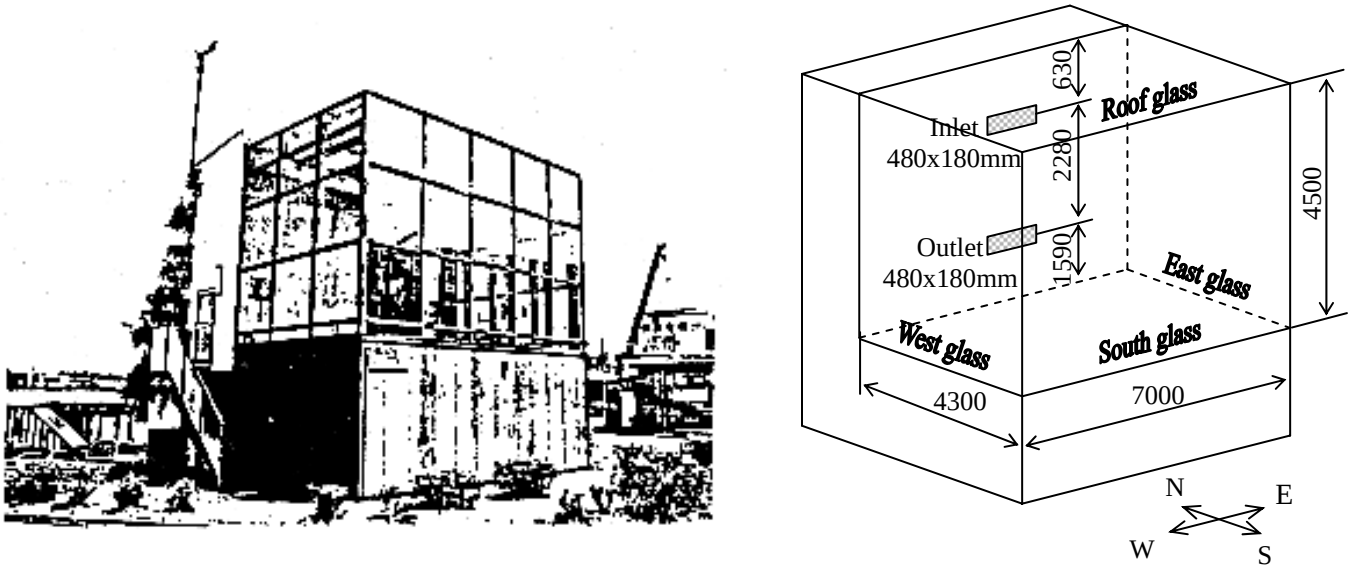


(a) (b)

Figure 9. The atrium used in the study. (a) The appearance of the experimental atrium, (b) the atrium size and openings (dimensions given in mm).

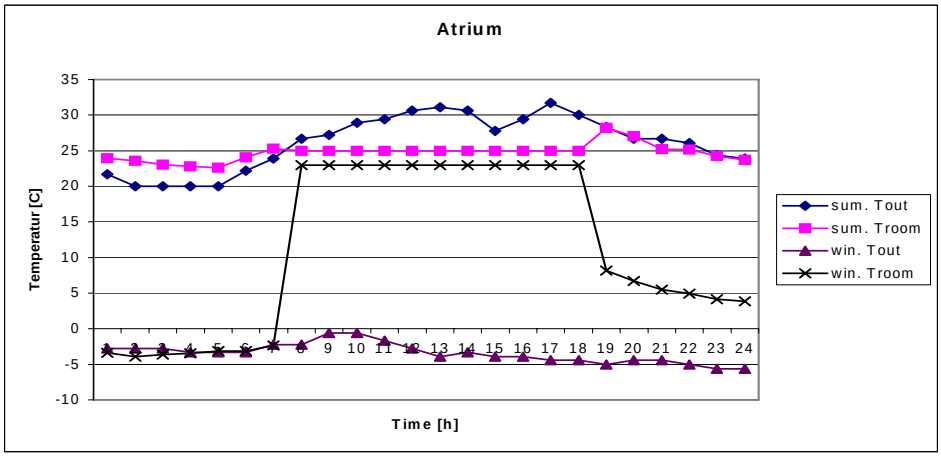


(a)

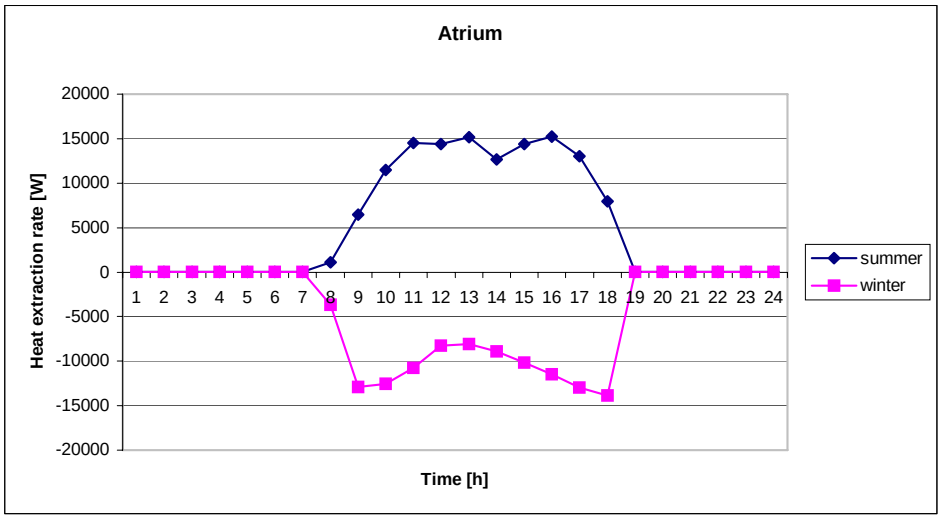


(b)

Figure 10. The climate data and results calculated by the coupled program for the house for the winter and summer days. (a) Indoor and outdoor air temperature, (b) heat extraction rate.

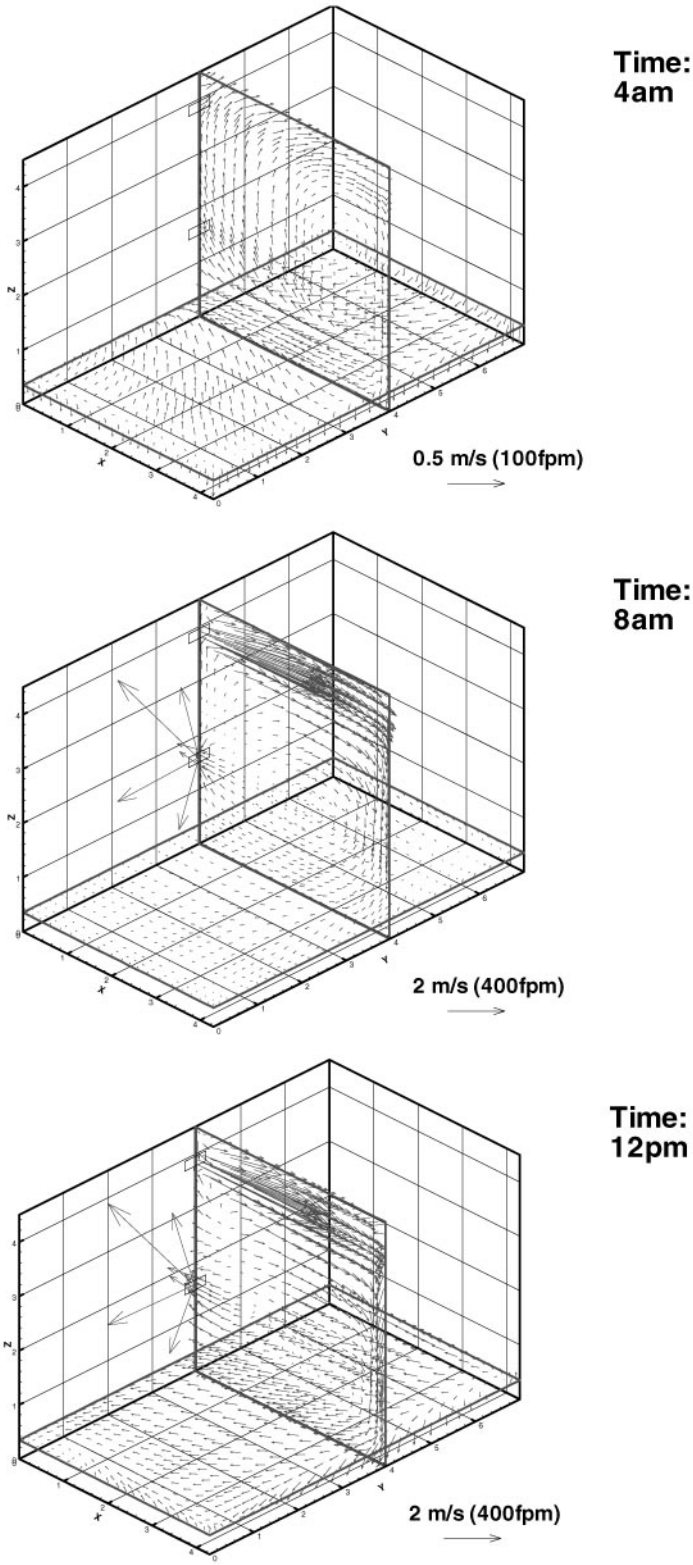


Figure 11. The computed air velocity distributions for the atrium during the summer day.

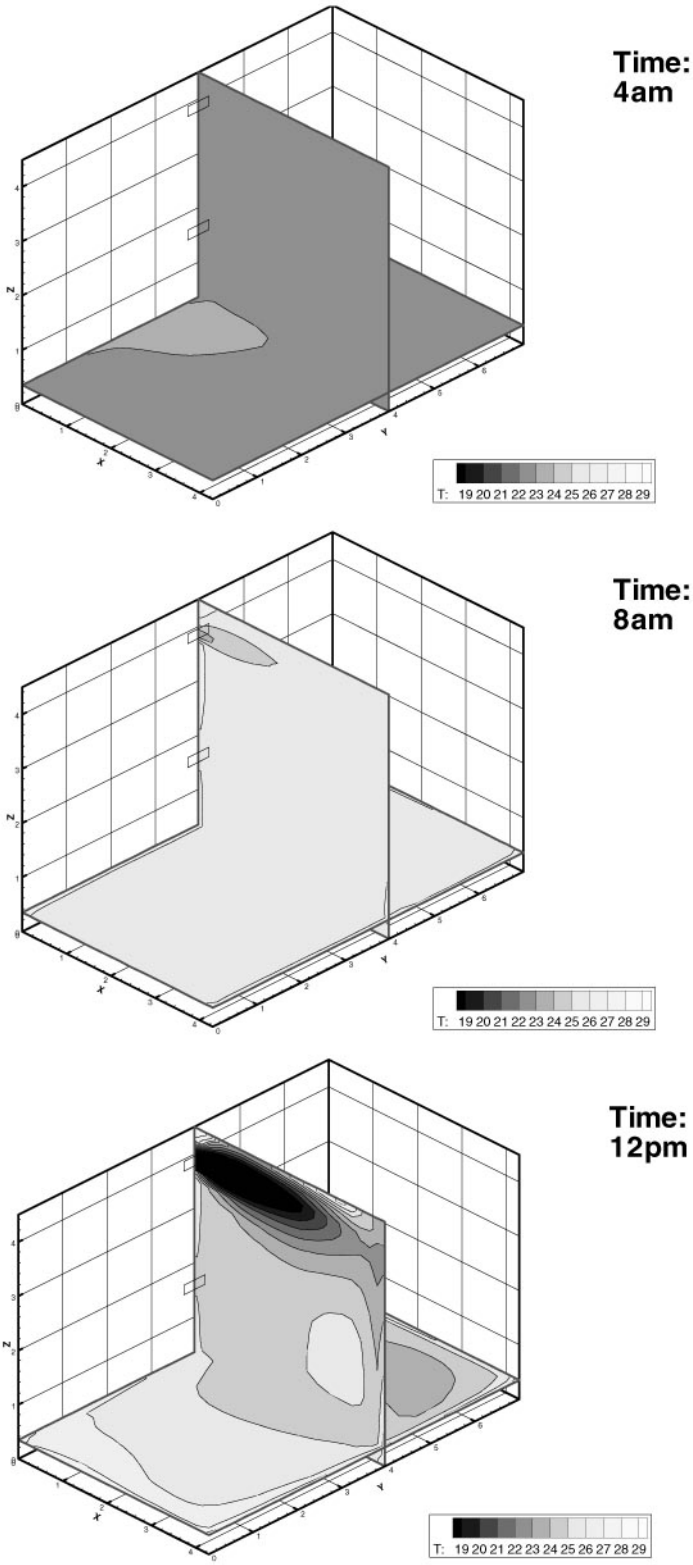


Figure 12. The computed air temperature distributions for the atrium during the summer day.

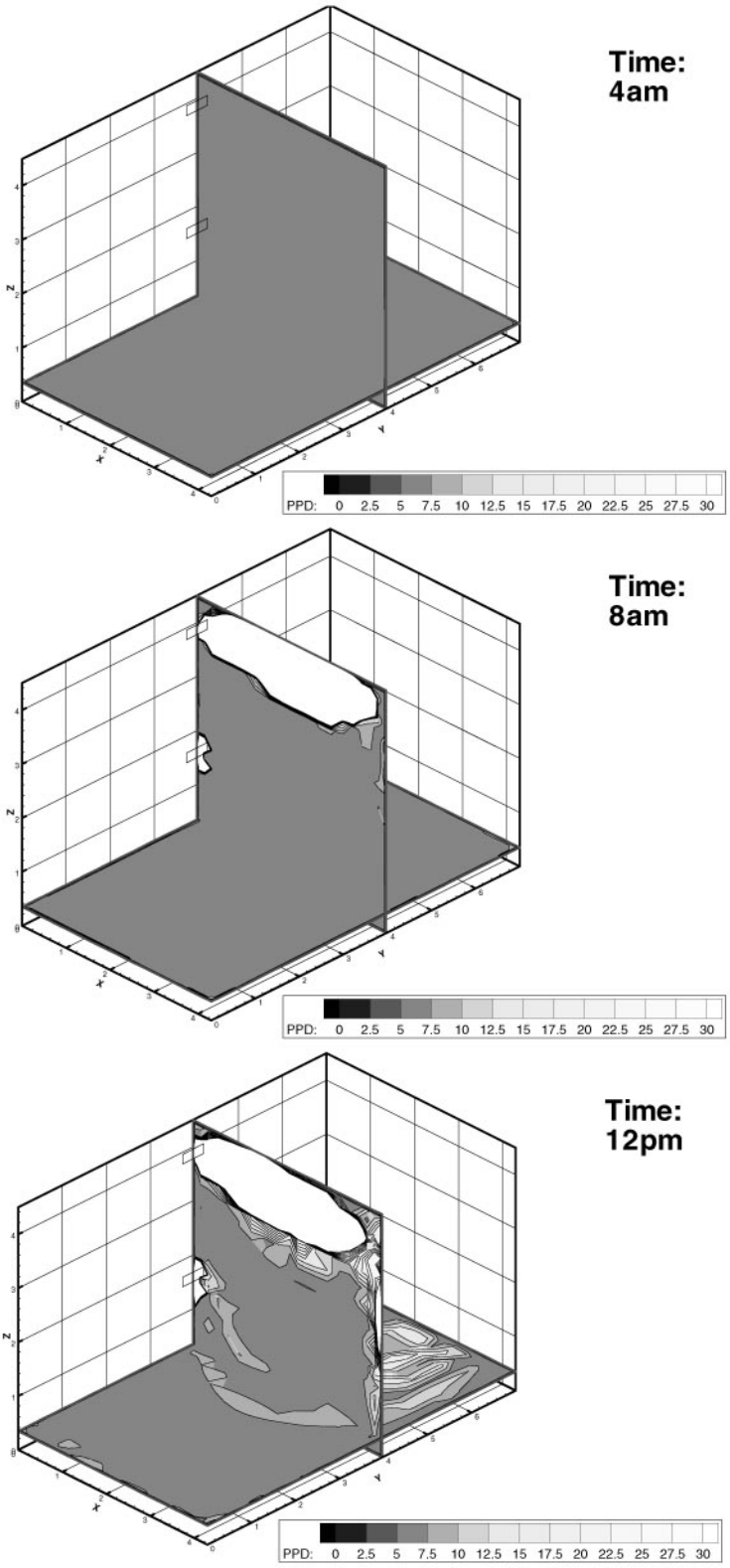


Figure 13. The predicted percentage dissatisfied distributions for the atrium during the summer day.